Electronic structure of random Ag-Pd and Ag-vacancy overlayers on a fcc Pd(001) substrate

M. V. Ganduglia-Pirovano
Corporate Research Science Laboratories, Exxon Research and Engineering Company, Annandale, New Jersey 08801

J. Kudrnovský
Institute of Physics, Czech Academy of Sciences, CS-180 40 Prague 8, Czech Republic

I. Turek
Institute of Physical Metallurgy, Czech Academy of Sciences, CS-616 62 Brno, Czech Republic

V. Drchal
Institute of Physics, Czech Academy of Sciences, CS-180 40 Prague 8, Czech Republic

M. H. Cohen
Corporate Research Science Laboratories, Exxon Research and Engineering Company, Annandale, New Jersey 08801 and Instituut voor Theoretische Fysica, Universiteit van Amsterdam, 1018 XE Amsterdam, The Netherlands
(Received 29 October 1992; revised manuscript received 19 March 1993)

The electronic structure and properties of two different types of random Ag overlayers on a nonrandom Pd(001) substrate have been studied. One overlayer is an Ag-Pd alloy and the other is Ag plus vacancies. Calculations were performed by means of a self-consistent, surface Green's-function technique based on the tight-binding linear-muffin-tin-orbital theory. The disorder was included via the coherent-potential approximation generalized to inhomogeneous systems. The layer-resolved local densities of states and the work functions were obtained.

I. INTRODUCTION

Adsorption of metal atoms on metal surfaces is a field of common interest to subjects such as the physics of two-dimensional systems, the growth of metal superlattices, alloying, etc. It is of practical importance for corrosion and heterogeneous catalysis and other processes for which control of surface constitution and properties is essential.

In a recent experiment[1] Petersson, Dannetun, and Lundström, have studied how Ag overlayers affect the hydrogen adsorption and desorption properties of Pd by means of ultraviolet photoemission spectroscopy (UPS). They investigated two types of Ag-covered Pd surfaces, the film-type, where all Ag atoms are located on the top of the Pd surface, and the alloy type, where Ag and Pd atoms are mixed in the surface layer. They reported that, in the film-type overlayer, the Pd 4*d* band is unaffected by the presence of Ag, while in the alloy type a significant reduction of intensity at the Fermi level in the Pd 4*d* band can be observed. However, their interpretation of the results for the desorption rates was independent of the variations in the Pd 4*d* band, in contradiction with the results presented in Ref. 2, where the importance of these electronic effects for hydrogen dissociation is stressed.

These experiments have motivated the present self-consistent calculations of the electronic properties of the two different types of random overlayers on a nonrandom fcc Pd(001) substrate, namely the AgPd-mixed alloy layer and an overlayer of Ag with vacancies. We use a recently developed first-principles approach[3,4] to calculate the electronic structure of a random overlayer on nonrandom substrates. The approach employs the tight-binding version of the linear muffin-tin orbital (TB-LMTO) method within the local-density approximation (LDA) to the density-functional formalism and the coherent-potential approximation (CPA) generalized to inhomogeneous systems to describe the effect of the disorder. The true semi-infinite nature of the system is incorporated via the surface Green's-function formalism.

In Sec. II the basic ideas of the method are briefly described. In Sec. III results for the two types of random overlayers on fcc Pd(001) are presented, and conclusions and comments are discussed in Sec. IV.

II. FORMALISM

The details of the self-consistent *ab initio* method for describing the electronic structure of disordered overlayers on metal substrates have been described elsewhere.[3,4] The main features of the method are the following. (i) The application of the TB-LMTO method[5] to describe the electronic structure from first principles. (ii) The use of the surface Green's-function formalism as re-

quired by the combined effect of alloy disorder and semi-infinite geometry.[6] The alloy disorder is included via the coherent-potential approximation generalized to inhomogeneous systems such as surfaces.[7] (iii) The system is considered as composed of three parts: (a) a semi-infinite ideal homogeneous bulk alloy, (b) a homogeneous vacuum represented by empty spheres with flat potentials, and (c) an intermediate region consisting of several atomic layers where all inhomogeneities (chemical, structural, and electronic) are concentrated. The latter contains also a few layers of empty spheres representing the vacuum-sample interface. The surface Green's functions are used to decouple the intermediate region from the semi-infinite vacuum and from the substrate bulk alloy. (iv) The Hartree and exchange potentials within the spheres are calculated via the atomic sphere approximation (ASA), while both monopole and the dipole terms of the charge density are included in the calculation of the Madelung potential.[8]

In order to calculate the electronic structure and properties of the described system, its configurationally averaged Green's function

$$\bar{g}(z) = \langle [P(z) - S]^{-1} \rangle = [\mathcal{P}(z) - S]^{-1} \tag{1}$$

needs to be determined. The quantity $g(z)$, which we term a Green's function, is related by a scaling transformation to the conventional or physical Green's function defined as the resolvent of the Kohn-Sham equations. It is more convenient than the conventional one for computation within our formalism.[3] In Eq. (1), $P(z)$ is a site-diagonal potential function matrix which characterizes the scattering properties of atoms placed at lattice sites. In the overlayer A_xB_{1-x} the potential function randomly takes two different values. Within the LDA and CPA, the nonrandom coherent-potential function matrix $\mathcal{P}(z)$, which is also a site diagonal quantity, is

$$\mathcal{P}(z) = \begin{cases} \mathcal{P}_p(z), & p = 1, 2, \ldots M, \text{ in the intermediate region} \\ P^b(z) \text{ or } P^v(z) & \text{otherwise,} \end{cases} \tag{2}$$

where the indices b and v refer to bulk and vacuum, respectively, and M is the number of layers in the intermediate region. In the present case the CPA self-consistency condition is restricted to the overlayer. We note that this random overlayer and the nonrandom layers in the intermediate region (including the layers of empty spheres) are all coupled together due to the LDA self-consistency. The potential function of the bulk substrate $P^b(z)$ is determined using the self-consistent TB-LMTO method.[9,10] For the cubic lattices with one atom per unit cell studied in this work, $P^b(z)$ is a diagonal matrix with respect to the site index and to the angular momentum index $L = (l, m)$. Due to the lowering of the symmetry at the surface, $\mathcal{P}(z)$ is nondiagonal with respect to the angular momentum index L. The quantity S refers to the screened structure constant within the most localized MTO representation.[11] It does not depend on the identity of the atoms, i.e., S is a nonrandom quantity, and it needs to be evaluated only once for a given surface. It has been found that within this representation and for closed-packed lattices, S is negligible beyond the first-nearest-neighbor shell (fcc lattice) or the second-nearest-neighbor shell (bcc lattice).[5] This property greatly facilitates the evaluation of the surface Green's function of the system and allows the use of the concept of the principal layer[12] (PL) defined in such a way that the semi-infinite system can be described by a stack of PL's with only nearest-neighbor PL's being coupled by the structure constants. Depending on the lattice structure and the surface orientation, a PL consists of one or more atomic layers. For fcc (001) surfaces and within the most localized MTO representation, a PL is equivalent to one atomic layer.[6] In addition, the relaxation of the top sample layer separations away from the ideal bulk interlayer distances will not be considered. We can then use the ideal bulk structure constant for both the bulk and the surface problems.

The central quantity, which enters both the CPA and LDA parts of the problem, is the on-site element of the conditionally averaged physical Green's function which is closely related to the configurationally averaged Green's function $\bar{g}(z)$, Eq. (1). Details concerning its evaluation can be found in Refs. 3 and 4.

The all-electron charge density within the individual atomic sphere centered at a lattice site and occupied by an atom of either type can be easily evaluated if one knows (i) the layer- and atom-resolved density of states matrix, which is related directly to the imaginary part of the on-site elements of the conditionally averaged physical Green's function,[7,10] and (ii) the radial solutions of the Schrödinger equation (normalized to unity within a given atomic sphere) corresponding to the spherical LDA potential

$$V_p^\alpha(|r|) = -2\frac{Z^\alpha}{|r|} + V_p^{\alpha,H}(\tilde{\rho}_p^\alpha(r)) + V_p^{\alpha,\mathrm{xc}}(\tilde{\rho}_p^\alpha(r)) + \sum_L \sum_q M_{pq}^{sL} \bar{Q}_q^L, \tag{3}$$

where

$$\bar{Q}_p^L = \sum_{\alpha=A,B} c_p^\alpha \left\{ \frac{\sqrt{4\pi}}{2l+1} \int_0^{s^\alpha} Y_L(\hat{r})\, |r|^l\, \rho_p^\alpha(r)\, dr - Z^\alpha \delta_{l,0} \right\}. \tag{4}$$

Here the Z^α denote the atomic numbers, and the first term in Eq. (3) represents the potential from the nuclei. The second and third terms are the Hartree and exchange-correlation contributions to the potential, re-

spectively. The tilde indicates that the spherically symmetric part of the charge density is used as in the ASA approach.[11] Finally, the last term describes the electrostatic potential acting on electrons in the pth layer due to the redistribution of electron density among layers in the intermediate region, i.e., the intersphere contribution to the spherically symmetric part of the one-electron potential. This redistribution of the electronic charge near the surface gives rise to the electrostatic (dipole) barrier $\Delta\phi$, which strongly affects the surface electronic structure. In order to describe the effect of the highly nonspherical charge density at the surface, it is necessary to include not only the monopole $\bar{Q}_p^{L=s}$ $(l=0, m=0)$ but also the dipole $\bar{Q}_p^{L=z}$ $(l=1, m=0)$ contributions to the multipole potential. The scheme used in Ref. 8 to evaluate these contributions has been modified to account for the disorder, which requires the statistical averaging of the multipole moments in each layer [see Eq. (4)]. The evaluation of the multipole matrices M_{pq}^{sL} requires a two-dimensional Ewald technique.

III. RESULTS

As discussed in the Introduction, the formalism is applied to the study of the electronic structure and properties of the disordered overlayers of Ag-Pd and Ag with vacancies on the Pd(001) substrate. The vacancies are represented by empty spheres with flat potentials determined self-consistently as in the case of Pd atoms. The model assumes that all interatomic distances within the overlayer, as well as between the layers of the intermediate region, are the same and equal to those in the Pd substrate. This is the case of an ideal epitaxially grown overlayer. The intermediate region consists of the disordered overlayer, two substrate layers, and two layers of empty spheres simulating the vacuum. In this region the potentials are varied until self-consistency is obtained with respect both to the LDA and CPA. For the exchange-correlation potential, the functional of Ceperley and Alder[13] as parametrized by Perdew and Zunger[14] is used. For k-space integration 21 special $k_{||}$ points[15] in the irreducible part of the surface Brillouin zone (SBZ) of the fcc(001) face are used, but for the evaluation of the layer-resolved density of states (DOS) 55 special $k_{||}$ points are used. The Fermi level E_f of the system is that of the substrate bulk as obtained from a self-consistent bulk TB-LMTO calculation.[11] As in Ref. 3, the Green's function of the bulk is constructed using the surface Green's function of the substrate. In this way the same $k_{||}$-space integration is used for both the bulk and surface cases. In each iteration loop, one CPA and one LDA step are performed. Self-consistency is considered to be achieved when the maximum differences among the input and output potentials in the intermediate region are below 0.01 Ry, which corresponds to at least mRy accuracy in the calculated eigenvalues.

Charge neutrality in the intermediate region as a whole is preserved within an accuracy of $10^{-3}e$. The number of electrons per atom belonging to the second Pd substrate layer, i.e., the third sample layer, was close to 10 within an accuracy of 10^{-3} in all cases. Also, for that layer the calculated dipole moments, which can be taken as a measure of the charge nonsphericity, were essentially zero within the same accuracy. Similar results were obtained for PdAg on Ag(001).[3] Due to the finite height of the surface dipole barrier, which characterizes the sample-vacuum interface, some charge is found outside the sample in the vacuum, typically $0.25e$.

The work function W was calculated using the expression $W = \Delta\phi - E_F$, where $\Delta\phi$ denotes the electrostatic dipole barrier across the surface and E_F is the Fermi level of the bulk substrate. The value of 5.84 eV for the clean Pd(001) surface compares well with the most recent experimental value of 5.8 eV.[17] Other experimental values of 5.0 eV and 5.3 eV have also been reported.[18,16] A calculated value of 5.0 eV was obtained using the self-consistent local orbital (SCLO) method for a seven-layer slab and three $k_{||}$ points.[16]

Let us now discuss the case of a silver monolayer on the Pd(001) substrate. Our computed value of W (see Table I) is 5.07 eV, and it should be compared with a value of 4.4 eV (Ref. 18) obtained using the SCLO method.[16] The available experimental value obtained from the angle-resolved photoemission measurements is 4.6 eV;[18] the same experiment yields a lower value of W for Pd(001), 5.0 eV, so that the decrease of work function due to the Ag monolayer coverage is 0.4 eV. Both theoretical calculations (the present method and the SCLO method of Refs. 16 and 18) give a similar decrease, 0.77 eV and 0.6 eV, respectively. A similar decrease of 0.6 eV of the work function due to the silver monolayer coverage was measured recently[19] for the Pd(110) surface.

The values of work functions of a random Ag_xPd_{1-x} overlayer on the Pd(001) substrate obtained by us are summarized in Table I. They decrease monotonically, but not linearly with the Ag content. Note that the opposite trend was found for the related case of the Ag-Pd overlayer on the Ag(001) substrate.[3] This is in accordance with a greater value of W for Pd as compared with Ag. No experimental result has been reported for the random overlayer on the fcc(001) face.

We have also performed calculations of the work function for the clean Ag(001) surface with (i) all distances equal to that of bulk Ag and (ii) with all distances equal

TABLE I. Calculated work functions for a clean Pd(001) surface and for an Ag_xPd_{1-x} random overlayer on a Pd(001) substrate.

Clean Pd(001) (eV)	$Ag_{25}Pd_{75}$ on Pd(001) (eV)	$Ag_{50}Pd_{50}$ on Pd(001) (eV)	$Ag_{75}Pd_{25}$ on Pd(001) (eV)	Monolayer of Ag on Pd(001) (eV)
5.84	5.71	5.56	5.36	5.07

to that of bulk Pd. This sequence of calculations permits one to examine the effect of the 5% compression of the Ag lattice on the work function. The computed values are (i) 4.78 eV and (ii) 5.05 eV, respectively. The former agrees well with the most recent experimental value of 4.64 eV for Ag(001).[20] The compressed Ag lattice value agrees well with the value of 5.07 eV obtained for the Ag monolayer case on Pd(001) (see Table I). A similar result was obtained for Pd on Ag(001), for which the work function was nearly the same as for expanded pure Pd.[3] These results together suggest that the value of the work function is largely determined by the outermost layer in these systems. It would be of great interest to learn how general this result is.

Let us comment briefly on the different values of work function obtained by different theoretical methods. There are two possible sources of discrepancies: (i) The slab geometry cannot avoid the interaction of the two surfaces through the few atomic layers included. We find that the bulk density of states is essentially reached in the fourth layer from the surface (Ref. 3 and the present work) in a semi-infinite material. The fourth layer is the central layer in the seven layer slab and is still sensitive to the slab boundary conditions.[16] Another problem with the slab geometry is the absence of true bulk states which are, among others, important for the proper determination of the Fermi level, a bulk property. The Green's-function techniques are based on the true semi-infinite geometry and are free of the above limitations. (ii) On the other hand, the slab methods, which employ the standard band-structure techniques, avoid the shape approximations for potentials or charge densities of the ASA. The full-potential treatment may be important for the dipole barrier determination, and the Green's-function techniques can only treat it in an approximate manner (as done in the present work). Note that the work function is determined by both the dipole barrier and the bulk Fermi level.

Similarly, the experimental determination of the work functions suffers from several problems. We first mention the fact that most measurements are performed on the polycrystalline samples rather than on the single crystal faces for which the calculations are done. Another problem concerns the quality of the sample surface. Surface roughness can lower the work function as discussed in Ref. 3. Diffusion of adsorbed atoms into the substrate can modify the results for adatom covered surfaces. Taking into account all these facts, the agreement between the different theoretical approaches on the one side, with the available experimental data on the other, can be considered to be satisfactory.

The results for the layer-resolved density of states are presented in Fig. 1 for the case of a clean Pd(001) surface, in Fig. 2 for a random $Ag_{50}Pd_{50}$ overlayer on Pd(001), and in Fig. 3 for a random $Ag_{50}Vac_{50}$ overlayer on Pd(001). The result for the Ag monolayer case is shown in Fig. 4. In all Ag-covered cases the result for the clean Pd(001) surface is presented as well for comparison.

In general, the shape and the width of the DOS of the second layer of the substrate agree well with the corresponding bulk result, computed within a bulk TB-LMTO approach.[9,10] This justifies our choice of the three sample layers in the intermediate region. On the other hand, the surface-layer DOS ($s1$) in Fig. 1, is distinctly narrower and, compared to the bulk, has a higher density about 1 eV below the Fermi level. The narrowing is expected

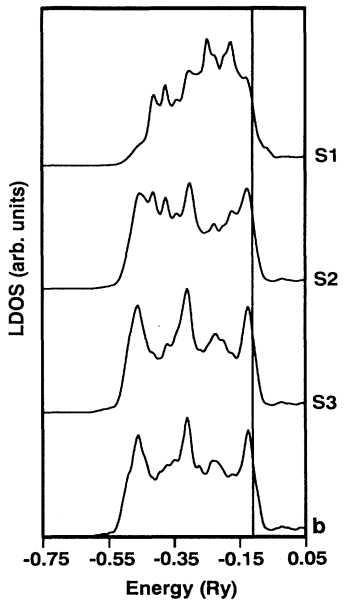

FIG. 1. Layer-resolved DOS's for a clean Pd(001) surface. The top three layers are denoted by $s1$, $s2$ and $s3$, while b refers to the bulk layer. The vertical line denotes the position of the bulk substrate Fermi level.

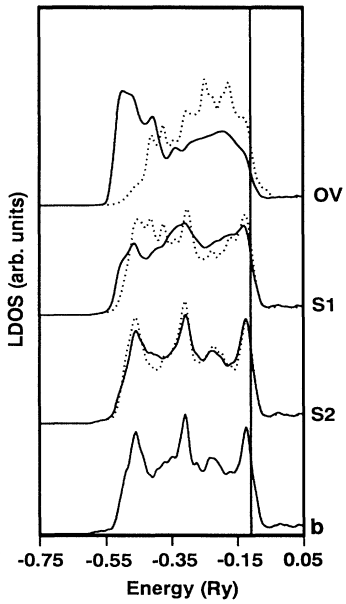

FIG. 2. Layer-resolved DOS's for an overlayer (ov) of random $Ag_{50}Pd_{50}$ on a Pd(001) surface. The two first layers of the substrate are denoted by $s1$ and $s2$, while b refers to the bulk layer. The corresponding results for a clean Pd(001) surface (dotted line) are shown. The vertical line denotes the position of the bulk substrate Fermi level.

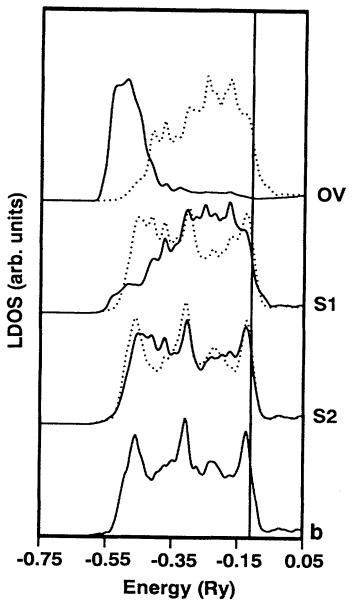

FIG. 3. Same as in Fig. 2, but for an overlayer of random $Ag_{50}Vac_{50}$ (Vac denotes a vacancy).

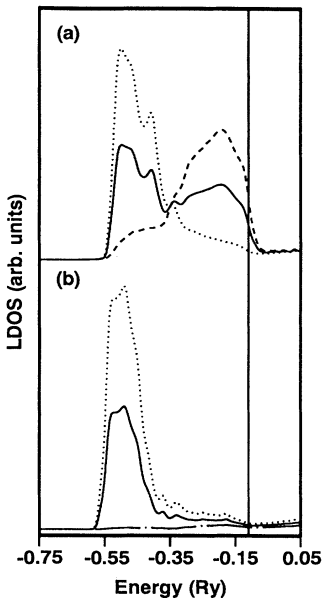

FIG. 5. Layer- and site-resolved DOS's for an overlayer of random (a) $Ag_{50}Pd_{50}$ and (b) $Ag_{50}Vac_{50}$ on a Pd(001) surface. The componentlike DOS's for Ag (dotted line), Pd (dashed line), and the vacancy (dash-dotted line) are shown. The vertical line denotes the position of the bulk substrate Fermi level.

because at the surface the number of nearest neighbors is reduced (the surface and bulk atoms have coordination 8 and 12, respectively). These findings agree well with the results of a self-consistent calculation using the slab method.[16]

The presence of the Ag atoms in the surface layer manifests itself in a well-separated extra peak [Figs. 5(a) and 5(b)] at the lower Pd d-band edge. The Ag- and Pd-related features are well separated from each other in energy, the Pd d-like states are strongly suppressed in the energy region of the Ag d-like states. The positions and widths of the d bands are in fairly good agreement with experimental results.[1] This behavior is qualitatively the same as that found in the corresponding $Ag_{50}Pd_{50}$ bulk alloy case.[7] Petersson, Dannetun, and Lundström[1] concluded from their UPS measurements of both type of Ag-covered surfaces that in the film-type case the Pd valence band is not affected by the presence of the Ag atoms in the surface. Of course, Pd d states are not seen in the calculated $Ag_{50}Vac_{50}$ DOS for the overlayer, but are seen in the experimental spectra for the corresponding surface type since the experiment samples several solid layers. The resolution of the experimental data is somewhat poor for a direct comparison with the calculated spectra. Nevertheless, one should notice that the total first substrate (s1) layer DOS for both types of overlayers (Figs. 2 and 3) is distinctly different; the presence of the Ag-atoms in the $Ag_{50}Vac_{50}$ overlayer is almost not reflected in the layer beneath. Note that the first substrate layer DOS for the $Ag_{50}Vac_{50}$ overlayer is very similar to the corresponding clean Pd(001) surface DOS. This gives evidence in favor of Petersson's conclusions.

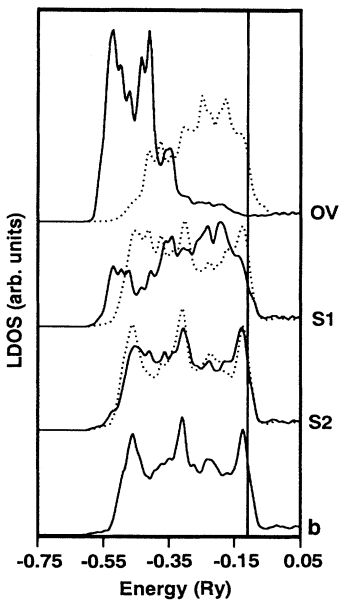

FIG. 4. Same as in Fig. 2, but for an Ag monolayer on Pd(001).

It is of interest to discuss the case of $Ag_{50}Vac_{50}$ overlayer in some detail. A vacancy represents a strong perturbation (the vacancy d states are typically 3 Ry above the Ag d states) which requires proper treatment (the rigid-band model or the virtual-crystal approximation are not applicable). A vacancy thus effectively removes the d states from a common alloy band. As a result, the overlayer DOS for $Ag_{50}Vac_{50}$ case has thus one-half of

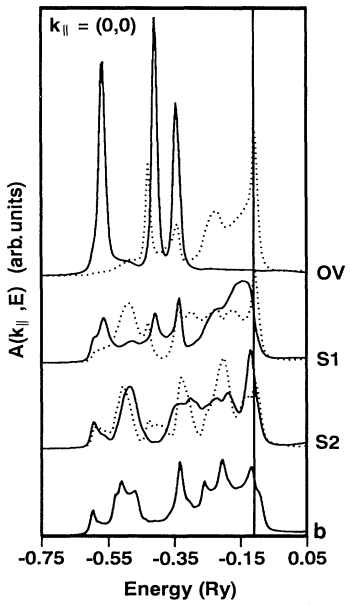

FIG. 6. Spectral layer-resolved DOS's for an Ag monolayer on a Pd(001) surface. The two first layers of the substrate are denoted by $s1$ and $s2$, while b refers to the bulk layer. The corresponding results for a clean Pd(001) surface (dotted line) are shown. The vertical line denotes the position of the bulk substrate Fermi level.

states compared to the Ag monolayer case (see Figs. 3 and 4), and it is structureless due to the alloy disorder. Another interesting feature is the shape similarity of the total DOS of the first and of the second substrate layers for $Ag_{50}Vac_{50}$ overlayer (curves $s1$ and $s2$ in Fig. 3) and of the total DOS of first two top layers for a clean Pd(001) (curves $s1$ and $s2$ in Fig. 1). This indicates the formation of a new surface, namely that of a clean Pd(001), with the increase of the vacancy "concentration." Finally, we note that the case with vacancies can serve as a simple model of random surface roughness on a microscopic scale (see also Ref. 3).

The layer-resolved spectral densities $A(k_{||}, E)$ for the Ag monolayer on Pd(001) face are presented in Fig. 6 for the case $k_{||} = (0,0)$. We note the clearly pronounced Ag-related peaks in the overlayer spectral density at the lower part of the Pd d bands. In the energy region about 3 eV below the Fermi level, there are essentially no Ag states. We note the similarity with the bulk AgPd alloys[10] where the center of the Ag d band is situated below the center of the Pd d band. The attenuation of the Ag-related features deep into the substrate is less pronounced than for the densities of states, where essentially the second substrate layer was bulklike (see Fig. 4).

The spectral densities for $k_{||} = (0,0)$ are related to the normal angle-resolved photoemission spectra. There are several such measurements available in the literature for the case of the Ag monolayer on Pd(001) substrate.[18,21,22] Direct comparison is, however, obscured by the matrix-element effect (selection rules) not included in $A(k_{||}, E)$, as well as by the fact that the available data are partially k integrated. Indeed, the k-resolved spectra are similar to the angle-integrated spectra of Ref. 1. The latter, in turn, are related to the densities of states. Keeping this in mind, one can conclude that the present calculations agree reasonably well with the available photoemission data.

IV. CONCLUSIONS

It has been shown that the self-consistent Green's-function technique based on the LDA within the TB-LMTO-CPA method applied here is sufficiently accurate for the calculation of the properties of disordered overlayers on metal substrates. Here two possible types of random Ag-covered surfaces have been studied, namely the case of a AgPd surface alloy and the case of an incomplete Ag overlayer on the Pd(001) substrate. Good agreement with available experimental photoemission data was obtained. The calculated work functions for the clean and Ag-monolayer covered Pd(001) surface agree reasonably well with the theoretical calculations based on the slab geometry as well as with available experimental data. For a disordered monolayer we predict a monotonic but nonlinear decrease of work function with increasing Ag coverage.

The method allows for the consideration of even more complex situations occurring in experiments such as the study of the surface of a disordered alloy with possible segregation of one alloy component at the sample surface.[7] The present approach in conjunction with the generalized perturbation method[23] can provide the effective cluster interactions[24] needed for the study of the thermodynamics of surface ordering and segregation phenomena from first principles. The formalism can be extended to include the effect of layer and atomic relaxations as well as relativistic effects. The present demonstration of the quantitative utility and convenience of this method encourages us to pursue these further developments.

[1] L.G. Petersson, H.M. Dannetun, and I. Lundström, Phys. Rev. B **30**, 3055 (1984).
[2] M. El-Batanouny, M. Strongin, and G.P. Williams, Phys. Rev. Lett. **46**, 269 (1981).
[3] J. Kudrnovský, I. Turek, V. Drchal, P. Weinberger, N.E. Christensen, and S.K. Bose, Phys. Rev. B **46**, 4222 (1992).
[4] J. Kudrnovský, B. Wenzien, V. Drchal, and P. Weinberger, Phys. Rev. B **44**, 4068 (1991).
[5] O.K. Andersen, and O. Jepsen, Phys. Rev. Lett. **53**, 2571 (1984).
[6] B. Wenzien, J. Kudrnovský, V. Drchal, and M. Šob, J. Phys. Condens. Matter **1**, 9893 (1989).
[7] J. Kudrnovský, V. Drchal, and P. Weinberger, Phys. Rev. B **44**, 6410 (1991).
[8] H.L. Skriver, and N.M. Rosengaard, Phys. Rev. B **43**, 9538 (1991).

[9]J. Kudrnovský, V. Drchal, and J. Mašek, Phys. Rev. B **35**, 2847 (1987).
[10]J. Kudrnovský and V. Drchal, Phys. Rev. B **41**, 7515 (1990).
[11]O.K. Andersen, O. Jepsen, and M. Šob, in *Electronic Band Structure and its Applications*, edited by M. Yussouf (Springer-Verlag, Heidelberg, 1987), p. 1.
[12]F. Garcia-Moliner and V.R. Velasco, Prog. Surf. Sci. **21**, 93 (1986).
[13]D.M. Ceperley and B.J. Alder, Phys. Rev. Lett. **45**, 566 (1980).
[14]J. Perdew and A. Zunger, Phys. Rev. B **23**, 5048 (1981).
[15]S.L. Cunningham, Phys. Rev. B **10**, 4988 (1974).
[16]J.G. Gay, J.R. Smith, F.J. Arlinghaus, and T.W. Capehart, Phys. Rev. B **23**, 1559 (1981).
[17]J. Rogozik, J. Küppers, and V. Dose, Surf. Sci. **148**, L653 (1984).
[18]T.W. Capehart, R. Richter, J.G. Gay, J.R. Smith, J.C. Buchholz, and F.J. Arlinghaus, J. Vac. Sci. Technol. **264**, 1214 (1983).
[19]P. Pervan and M. Milun, Surf. Sci. **264**, 135 (1992).
[20]N.V. Smith, C.T. Chen, and M. Weinert, Phys. Rev. B **40**, 7565 (1989).
[21]M. Pessa, M. Vulli, and H. Asonen, Ann. Isr. Phys. Soc. **6**, 342 (1984).
[22]D.G. O'Neill, J.J. Joyce, T.W. Capehart, and J.H. Weaver, J. Vac. Sci. Technol. A **3**, 1639 (1985).
[23]F. Ducastelle and F. Gautier, J. Phys. F **6**, 2039 (1976); F. Treglia, B. Legrand, and F. Ducastelle, Europhys. Lett. **7**, 575 (1988).
[24]V. Drchal, J. Kudrnovský, L. Udvardi, P. Weinberger, and A. Pasturel, Phys. Rev. B **45**, 14 328 (1992).